Kenji Takizawa · Bradley Henicke · Darren Montes · Tayfun E. Tezduyar · Ming-Chen Hsu · Yuri Bazilevs

Numerical-Performance Studies for the Stabilized Space–Time Computation of Wind-Turbine Rotor Aerodynamics

Abstract We present our numerical-performance studies for 3D wind-turbine rotor aerodynamics computation with the Deforming-Spatial-Domain/Stabilized Space–Time (DSD/SST) formulation. The computation is challenging because of the large Reynolds numbers and rotating turbulent flows, and computing the correct torque requires an accurate and meticulous numerical approach. As the test case, we use the NREL 5MW offshore baseline wind-turbine rotor. We compute the problem with both the original version of the DSD/SST formulation and the version with an advanced turbulence model. The DSD/SST formulation with the turbulence model is a recently-introduced space–time version of the residual-based variational multiscale method. We include in our comparison as reference solution the results obtained with the residual-based variational multiscale Arbitrary Lagrangian–Eulerian method using NURBS for spatial discretization. We test different levels of mesh refinement and different definitions for the stabilization parameter embedded in the "least squares on incompressibility constraint" stabilization. We compare the torque values obtained.

Keywords DSD/SST formulation, Space–time variational multiscale method, Wind-turbine aerodynamics, Rotating turbulent flow, Torque values

Kenji Takizawa
Department of Modern Mechanical Engineering and Waseda Institute for Advanced Study, Waseda University
1-6-1 Nishi-Waseda, Shinjuku-ku, Tokyo 169-8050, JAPAN

Bradley Henicke, Darren Montes, Tayfun E. Tezduyar
Mechanical Engineering, Rice University – MS 321
6100 Main Street, Houston, TX 77005, USA
E-mail: tezduyar@rice.edu

Ming-Chen Hsu and Yuri Bazilevs
Structural Engineering, University of California, San Diego
9500 Gilman Drive, La Jolla, CA 92093, USA

1 Introduction

Wind-turbine rotor aerodynamics has become an application and testing area for some of the most advanced computational mechanics techniques. For example, two recent journal articles [1; 2] document how advanced computational fluid mechanics and fluid–structure interaction (FSI) techniques were used in the first comprehensive effort to simulate wind-turbine rotors in 3D at full scale, including rotor-geometry definition, meshing, aerodynamic and structural modeling, and fully-coupled FSI computation. Isogeometric analysis [3] was employed for the bulk of the computations reported in [1; 2]. Wind-turbine rotor aerodynamics also partially motivated the development of the most recent version of the Deforming-Spatial-Domain/Stabilized Space–Time (DSD/SST) formulation. The DSD/SST formulation was introduced in [4; 5; 6], was supplemented in [7] with advanced stabilization parameters, gained in [8] new versions with increased scope and robustness, and was elevated in [9] to a new version with an advanced turbulence model. This most recent DSD/SST formulation with the turbulence model is a space–time version [9] of the residual-based variational multiscale (VMS) method [10; 11; 12; 13]. It was successfully tested on wind-turbine rotor aerodynamics in [14].

Addressing the type of computational challenges involved in wind-turbine rotor aerodynamics has been a part of the computational mechanics research targeting flows with moving boundaries and interfaces (see, for example, [15; 16; 17; 18; 19; 20; 21; 22; 23; 24; 25; 26; 27; 28; 29; 30; 31; 32; 33; 34; 35; 36; 37; 38; 39; 40; 41; 42; 43; 44; 45; 8; 46; 47; 48; 49; 50; 51; 52; 53; 54; 55; 56; 57; 58; 59; 60; 61; 62; 63; 64; 65; 66; 67; 68; 69; 70; 71; 72; 73; 1; 2; 74; 75; 76; 77; 78; 79; 9; 80; 81; 82; 83]), including FSI and flows with mechanical components in fast, linear or rotational relative motion [22; 25; 28; 32; 59]. With the terminology used in [84], we can categorize a method for flow problems with moving boundaries and interfaces as an interface-tracking (moving-mesh) technique or an interface-capturing (nonmoving-mesh) technique, or a combination of the two. Comments on the advantages and disadvantages of these two categories of techniques and how they can be enhanced or combined were provided in [14], together with references [84; 28; 7; 85; 8; 86; 51] on these matters

The DSD/SST formulation is one of the earliest space–time techniques for moving boundaries and interfaces. Its stabilization components are the Streamline-Upwind/Petrov-Galerkin (SUPG) [87] and Pressure-Stabilizing/Petrov-Galerkin (PSPG) [4; 88] methods. The DSD/SST formulation, like most stabilized formulations, involves stabilization parameters that play an important role in determining the accuracy of the formulation. There are various ways of defining the stabilization parameters (see, for example, [89; 4; 90; 7; 91; 92; 93; 94; 95; 42; 96; 8; 97; 98; 99; 100]). The ones used with the DSD/SST formulation in recent years have mostly been those given in [7; 8], including the stabilization parameter embedded in the "least squares on incompressibility constraint (LSIC)" stabilization.

The new-generation DSD/SST formulations introduced in [8] were named "DSD/SST-SP", "DSD/SST-TIP1" and "DSD/SST-SV" to differentiate them from the original version introduced in [4; 5; 6], which was named "DSD/SST-DP" in [8]. The new formulations have been the core technologies of the stabilized space–time FSI (SSTFSI) technique, which was also introduced in [8]. The SSTFSI technique, supplemented with special FSI techniques targeting specific classes of problems, has been successfully applied to complex, real-world problems, such as computer modeling of the Orion Spacecraft parachutes (see [51; 52; 72; 75; 77; 80; 81]) and patient-specific modeling of cerebral aneurysms (see [43; 53; 60; 65; 67; 66; 76; 79; 82]).

The new DSD/SST formulation introduced in [9], which is the space–time version of the residual-based VMS method, was implemented specifically for DSD/SST-DP, and it was named in [9] "DSD/SST-DP-VMST" (implying the version with the VMS turbulence model). To differentiate it from this new version, the original DSD/SST-DP version was named in [9] "DSD/SST-DP-SUPS" (implying the version with the SUPG/PSPG stabilization). In [14], we tested the DSD/SST-DP-VMST formulation on wind-turbine rotor aerodynamics for the first time. The objective was to show that this new formulation gives a good torque value. In the numerical-performance studies we conduct in this paper for the DSD/SST computation of wind-turbine rotor aerodynamics, we use the DSD/SST-DP-VMST and DSD/SST-DP-SUPS formulations with different levels of mesh refinement and different definitions for the stabilization parameter embedded in the LSIC stabilization. In the test computations we use is the NREL 5MW offshore baseline wind-turbine rotor, with the geometry coming from [1]. We include in our comparison as reference solution the results obtained with the residual-based VMS ALE method using NURBS for spatial discretization.

The geometry of the wind-turbine rotor blade and hub is described in Section 2. The problem setup, mesh generation and computations are presented in Section 3. The concluding remarks are given in Section 4.

2 Geometry construction for the wind-turbine rotor blade and hub

The geometry construction for the wind-turbine rotor blade and hub we are using in the computations was described in [1; 14], and we provide some of that information here. The geometry of the rotor blade is based on the NREL 5MW offshore baseline wind turbine reported in [101]. A 61 m blade is attached to a hub with radius of 2 m, making the total rotor radius, R, 63 m. The blade is composed of several airfoil types (see Figure 1). The first portion of the blade is a perfect cylinder. Farther away from the root the cylinder is smoothly blended into a series of DU (Delft University) airfoils. Starting at 44.55 m from the root and all the way to the tip, the NACA64 is profile used. For each cross-section, we use quadratic

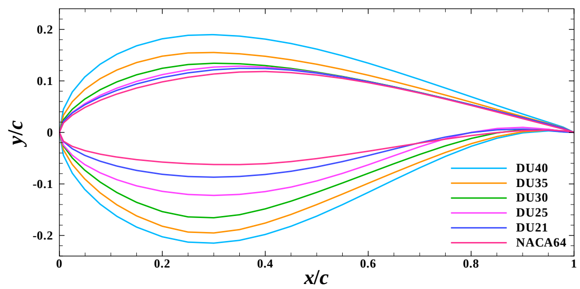

Fig. 1 Airfoil types used in the design of the wind-turbine rotor blade.

NURBS to represent the 2D airfoil shape. The weights of the NURBS functions are set to unity. The weights are adjusted near the root to represent the circular cross-sections exactly. The cross-sections are lofted along the blade axis direction, also using quadratic NURBS and unit weights. This geometry-construction process yields a smooth blade surface with a relatively small number of input parameters, which is an advantage of the isogeometric representation. The final blade shape is shown in Figure 2, together with the airfoil shapes. Figure 2 also shows the airfoils seen with a viewing direction parallel to the blade axis, and that illustrates the twisting of the cross-sections.

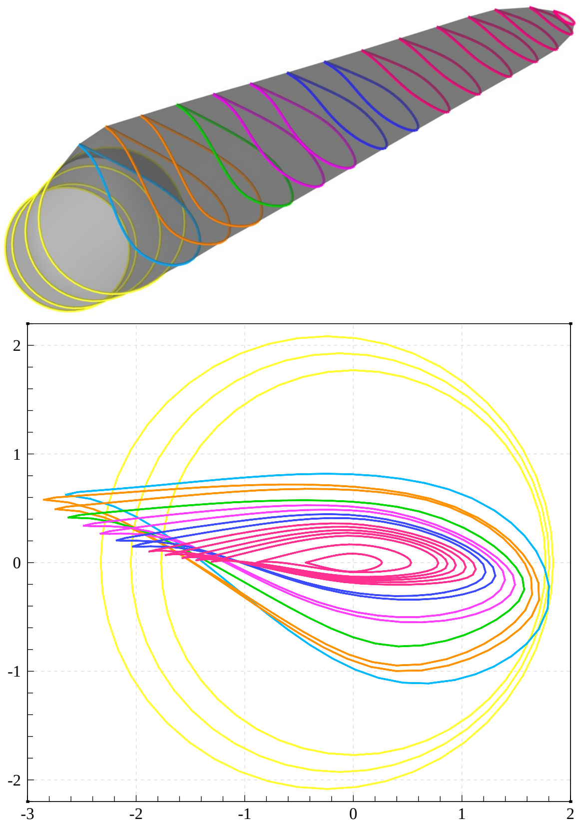

Fig. 2 Top: Airfoils superposed on the blade. Bottom: Airfoils seen with a viewing direction parallel to the blade axis, illustrating the twisting of the cross-sections. Axes units are meters.

3 Computation with the DSD/SST formulation

3.1 Problem setup and mesh generation

We compute the aerodynamics of the rotor, shown in Figure 3, with a prescribed shape and speed with a rotating mesh. The wind speed is uniform at 9 m/s and the rotor speed is 1.08 rad/s, giving a tip speed ratio of 7.55 (see [102] for wind-turbine terminology). We use air properties at standard sea-level conditions. The Reynolds number (based on the chord length at $\frac{3}{4}R$ and the relative velocity there) is approximately 12 million. At the inflow boundary the velocity is set to the wind velocity, at the outflow boundary the stress vector is set to zero, and at the radial boundary the radial and circumferential components of the velocity are set to zero.

3.2 Surface mesh

To generate the triangular mesh on the rotor surface, we started with a quadrilateral surface mesh generated by interpolating the NURBS geometry at each knot intersection. We subdivided each quadrilateral element into triangles and then made minor modifications to improve the mesh quality near the hub. We use three different meshes: Mesh-2, Mesh-3 and Mesh-4, with the surface mesh refined along the blade 2, 3 and 4 times, respectively, compared to the finite element mesh used in [1]. The number of nodes and elements for each blade surface mesh is shown in Table 1, and Figure 4 shows the surface mesh for Mesh-4.

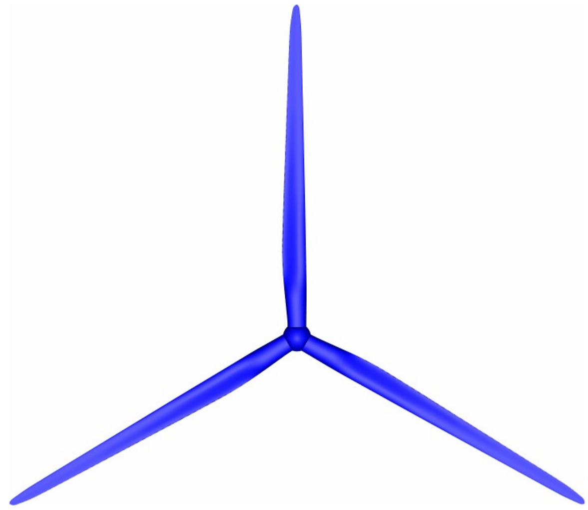

Fig. 3 Wind-turbine rotor.

3.3 Volume mesh

For computational efficiency, rotational-periodicity [75; 77] is utilized so that the domain includes only one of three blades, as shown in Figure 5. The inflow, outflow and radial boundaries lie $0.5R$, $2R$ and $1.43R$ from the hub center, respectively. This can be more easily seen in Figure 6, where the inflow, outflow, and radial boundaries are the left, right and top edges, respectively, of the cut plane along the rotation axis. Each periodic boundary contains 1,430 nodes and 2,697 triangles. Near the rotor surface, we have 22 layers of refined mesh with first-layer thickness of 1 cm and a progression factor of 1.1. The boundary layer mesh at $\frac{3}{4}R$ is shown in Figure 7.

	Surface		Volume	
	nn	ne	nn	ne
Mesh-2	5,748	11,452	155,494	898,640
Mesh-3	7,552	15,060	205,855	1,195,452
Mesh-4	9,268	18,492	253,340	1,475,175

Table 1 Summary of the meshes. Here nn and ne are the number of nodes and elements.

The number of nodes and elements for each volume mesh is shown in Table 1.

Fig. 4 Rotor surface mesh (Mesh-4).

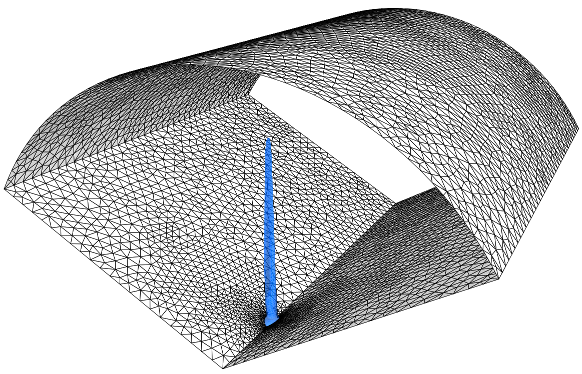

Fig. 5 Rotationally-periodic domain with wind-turbine blade shown in blue.

3.4 Computation

We compute the problem with the DSD/SST-DP-SUPS and DSD/SST-DP-VMST [9] techniques. For the VMST technique, we test both definitions of "ν_{C}" given in [9]. We will call the one given by Eq. (17) in [9] "TC2", and the one given by Eq. (18), "TGI". In addition, we use

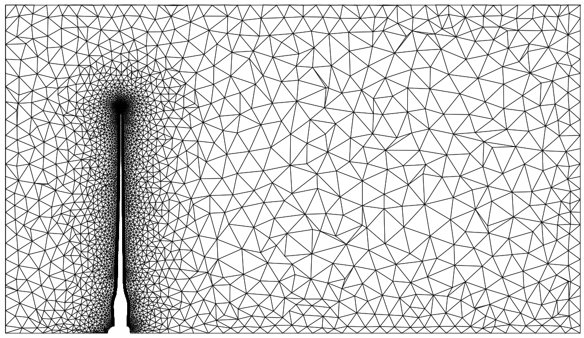

Fig. 6 Cut plane of the fluid volume mesh along rotor axis (Mesh-4).

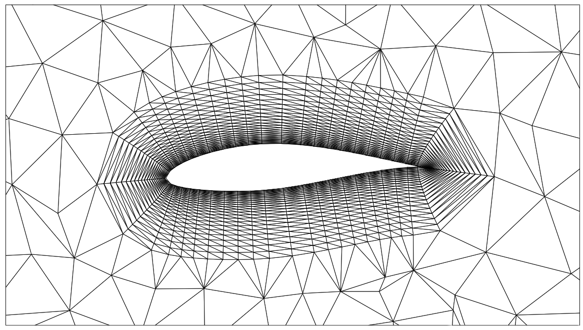

Fig. 7 Boundary layer mesh at $\frac{3}{4}R$.

the following definition of ν_{C}:

$$\nu_{\text{C}} = \left(\nu_{\text{LSIC}}^{-2} + \nu_{\text{HRGN}}^{-2}\right)^{-\frac{1}{2}}, \tag{1}$$

$$\nu_{\text{LSIC}} = \tau_{\text{SUPG}} \left\|\mathbf{u}^h - \mathbf{v}^h\right\|^2, \tag{2}$$

$$\nu_{\text{HRGN}} = \frac{h_{\text{RGN}}^2}{\tau_{\text{SUPG}}}, \tag{3}$$

where h_{RGN} is given by Eqs. (10) and (11) in [8]. We call this option "LHC".

Remark 1 *Eq. (3), which comes from [13], has been modified for compatiblity with other stabilization parameters.*

With the SUPS technique, we test two options, one with the "LSIC" stabilization, and one without. The computations are summarized in Table 2.

In solving the linear equation systems involved at every nonlinear iteration, the GMRES search technique [103] is used with a diagonal preconditioner. The computation is carried out in a parallel computing environment, using PC clusters. The mesh is partitioned to enhance the parallel efficiency of the computations. Mesh partitioning is based on the METIS algorithm [104]. The time-step size is 4.67×10^{-4} s. The number of nonlinear iterations per time step is 3 with 30, 60 and 500 GMRES iterations for the first, second and third nonlinear iterations, respectively.

Prior to the computations reported here, we performed a series of brief computations with the DSD/SST-DP-

Method	Stabilization	Mesh
SUPS	LSIC	Mesh-4
SUPS	No LSIC	Mesh-2
SUPS	No LSIC	Mesh-3
SUPS	No LSIC	Mesh-4
VMST	TGI	Mesh-2
VMST	TGI	Mesh-3
VMST	TGI	Mesh-4
VMST	TC2	Mesh-4
VMST	LHC	Mesh-4

Table 2 Summary of the computations.

SUPS technique, starting from a lower Reynolds number and gradually reaching the actual Reynolds number. This solution is used as the initial condition also for the computations with the DSD/SST-DP-VMST technique. The purpose is to generate a divergence-free and reasonable flow field at this Reynolds number. We note that it was especially difficult with the VMST option to start from non-physical conditions, such as setting all nodes except those on the blade to the inflow velocity.

3.5 Results

Figures 8–10 show the time history of the aerodynamic torque and the torque contribution from each patch for a single blade at $t = 1.0$ s. The patches are defined as shown in Figure 11.

Figures 12–14 show the pressure distribution on the suction side of the blade, near the tip. The torque is generated mostly by the lower pressure region, which is the bottom, smooth-colored region of the blade shown in the pictures. Figures 15–17 show the pressure coefficients at $t = 1.0$ s for Patch 16 (at $0.90R$), which is a representative section of the blade. For most of the patches, the angle of attack and Reynolds number do not vary much from one patch to another. For example, the angle of attack and Reynolds number are $7.6°$ and 9.6×10^6 for Patch 16 (at $0.90R$).

Remark 2 *As mentioned in [14], we believe that the torque level reached with the TC2 definition of ν_{C}, and now also with the LHC definition, may still not be unreasonable, because we are computing with a computational domain that extends only 1.43R in the radial direction. This calls for further investigation.*

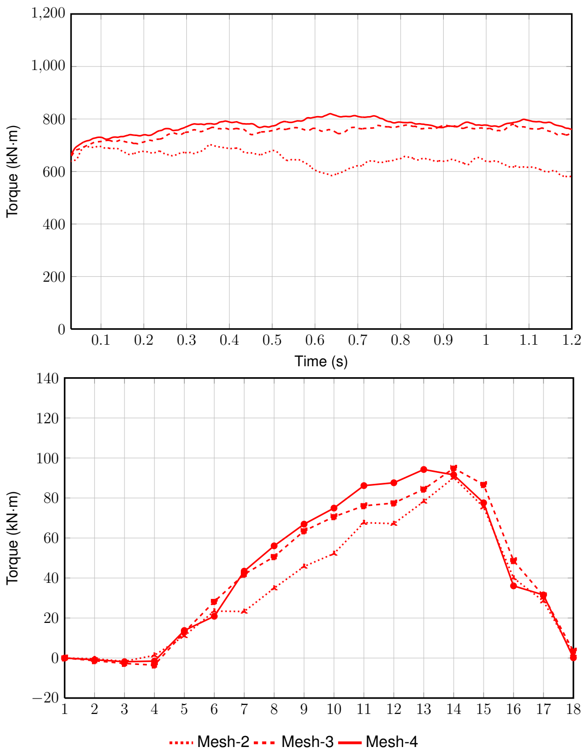

Fig. 8 The aerodynamic torque generated by a single blade. Comparison between different meshes with the DSD/SST-DP-SUPS technique. Time history (top). The torque contribution from each patch at $t = 1.0$ s (bottom).

3.6 Discussion

3.6.1 Surface-mesh refinement

Mesh refinement studies for both the SUPS and VMST techniques indicate good convergence. This is shown in Figures 8 and 9. We note that both the DSD/SST-DP-SUPS and DSD/SST-DP-VMST (TGI) techniques do not perform well with Mesh-2. Looking at Figures 12–13 and 15–16, we see larger pressure fluctuations for Mesh-2. This is an evidence of a larger vortex, which we believe to be caused by a lack of numerical stability.

3.6.2 SUPS with and without LSIC stabilization

As can be seen in Figure 10, the DSD/SST-DP-SUPS technique with LSIC stabilization does not perform well.

3.6.3 VMST with different ν_{C} definitions

The TC2 and LHC options yield very similar results, as opposed to the TGI option, which predicts significantly lower torque. We believe this to be mainly related to the stabilization near the boundary; while ν_{C} for the TC2 and LHC options goes to zero, it goes to larger and larger values for the TGI option as the time step size becomes smaller and smaller.

4 Concluding remarks

We have conducted numerical-performance studies for the DSD/SST computation of wind-turbine rotor aerodynamics. These computations are challenging because of the large Reynolds numbers and rotating turbulent

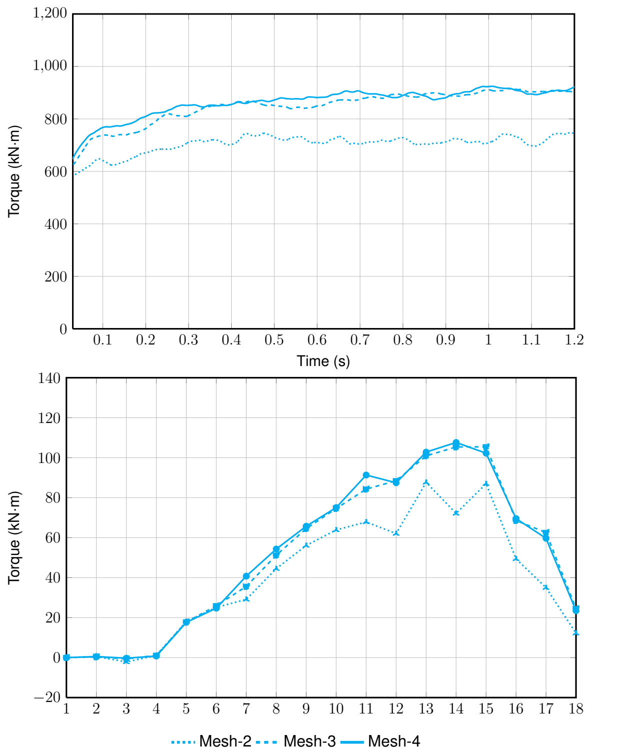

Fig. 9 The aerodynamic torque generated by a single blade. Comparison between different meshes with the DSD/SST-DP-VMST (TGI) technique. Time history (top). The torque contribution from each patch at $t = 1.0$ s (bottom).

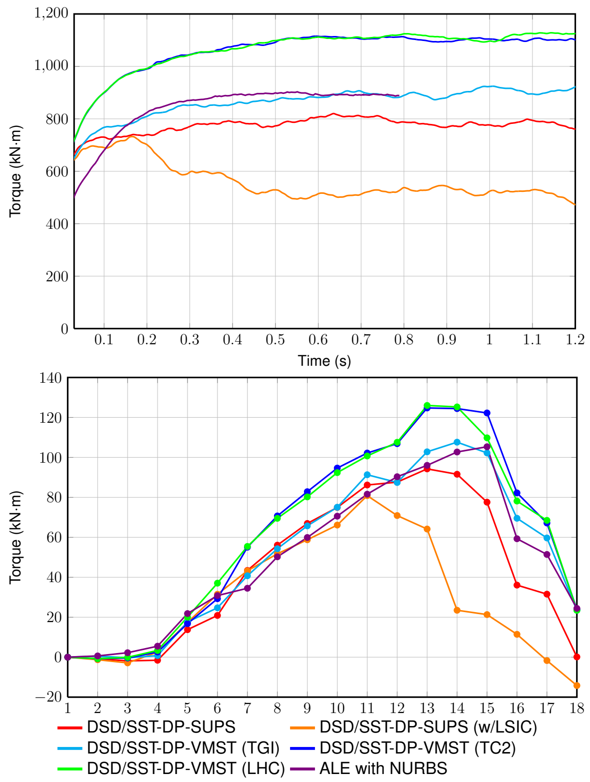

Fig. 10 The aerodynamic torque generated by a single blade. Computed with different techniques using Mesh-4. Time history (top). The torque contribution from each patch at $t = 1.0$ s (bottom). We note that the curve labeled “ALE with NURBS” is from [1] and corresponds to $t = 0.8$ s.

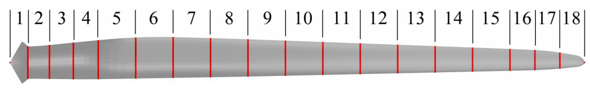

Fig. 11 Patches along the blade.

flows, and computing the correct torque requires much care. As the test case, we used the NREL 5MW offshore baseline wind-turbine rotor. We reported results obtained with both the original version of the DSD/SST formulation and the version with an advanced turbulence model. The original version is the DSD/SST-DP-SUPS formulation, which has the SUPG and PSPG stabilizations. The DSD/SST formulation with the turbulence model is a recently-introduced space–time version of the residual-based VMS method. We used these two formulations with different levels of mesh refinement and different definitions for the stabilization parameter embedded in the LSIC stabilization. We included in our comparison as reference solution the results obtained with the residual-based VMS ALE method using NURBS for spatial discretization.

Acknowledgment

This work was supported in part by the Rice Computational Research Cluster funded by NSF Grant CNS-0821727. Method analysis and evaluation components of this work were supported also in part by ARO Grant W911NF-09-1-0346. We thank Samuel E. Wright III whose previous work on this project contributed to mesh generation and data reduction. M.-C. Hsu and Y. Bazilevs were partially supported by the Los Alamos–UC San Diego Educational Collaboration Fellowship. Y. Bazilevs would also like to acknowledge the support of the Hellman Fellowship.

References

1. Y. Bazilevs, M.-C. Hsu, I. Akkerman, S. Wright, K. Takizawa, B. Henicke, T. Spielman, and T.E. Tezduyar, “3D simulation of wind turbine rotors at full scale. Part I: Geometry modeling and aerodynamics”, *International Journal for Numerical Methods in Fluids*, **65** (2011) 207–235, doi: 10.1002/fld.2400.
2. Y. Bazilevs, M.-C. Hsu, J. Kiendl, R. Wüchner, and K.-U. Bletzinger, “3D simulation of wind turbine rotors at full scale. Part II: Fluid–structure interaction modeling with composite blades”, *International Journal for Numerical Methods in Fluids*, **65** (2011) 236–253.
3. T.J.R. Hughes, J.A. Cottrell, and Y. Bazilevs, “Isogeometric analysis: CAD, finite elements, NURBS, exact geometry, and mesh refinement”, *Computer Methods in Applied Mechanics and Engineering*, **194** (2005) 4135–4195.
4. T.E. Tezduyar, “Stabilized finite element formulations for incompressible flow computations”, *Advances in*

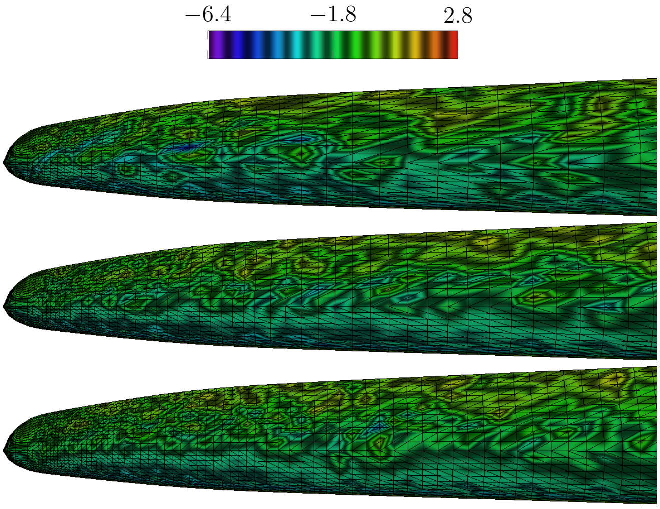

Fig. 12 Pressure (kPa) near rotor tip at $t = 1.0$ s computed with the DSD/SST-DP-SUPS technique. Top: Mesh 2. Middle: Mesh 3. Bottom: Mesh 4.

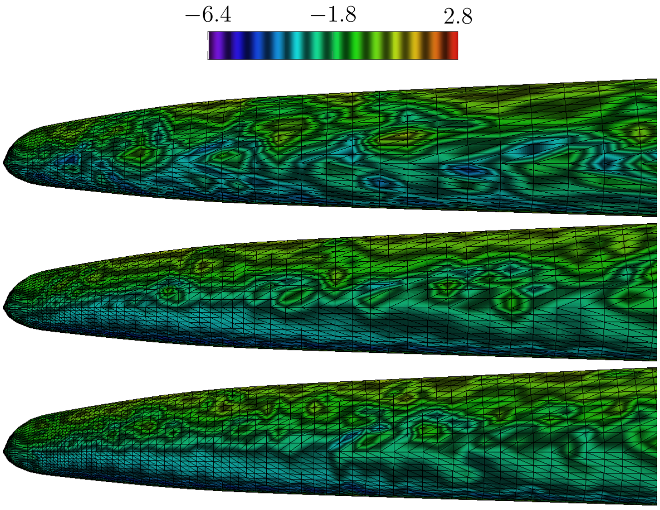

Fig. 13 Pressure (kPa) near rotor tip at $t = 1.0$ s computed with the DSD/SST-DP-VMST (TGI) technique. Top: Mesh 2. Middle: Mesh 3. Bottom: Mesh 4.

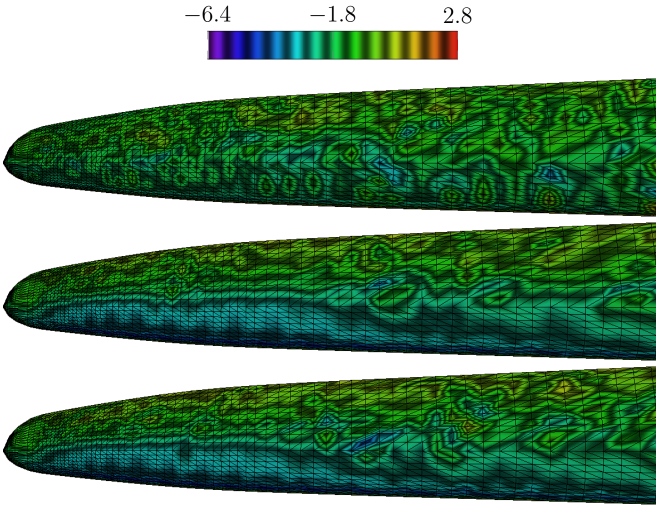

Fig. 14 Pressure (kPa) near rotor tip at $t = 1.0$ s computed with different techniques and Mesh-4. Top: DSD/SST-DP-SUPS (w/LSIC). Middle: DSD/SST-DP-VMST (TC2). Bottom: DSD/SST-DP-VMST (LHC).

Applied Mechanics, **28** (1992) 1–44, doi: 10.1016/S0065-2156(08)70153-4.
5. T.E. Tezduyar, M. Behr, and J. Liou, "A new strategy for finite element computations involving moving boundaries and interfaces – the deforming-spatial-domain/space–time procedure: I. The concept and the preliminary numerical tests", *Computer Methods in Applied Mechanics and Engineering*, **94** (1992) 339–351, doi: 10.1016/0045-7825(92)90059-S.
6. T.E. Tezduyar, M. Behr, S. Mittal, and J. Liou, "A new strategy for finite element computations involving moving boundaries and interfaces – the deforming-spatial-domain/space–time procedure: II. Computation of free-surface flows, two-liquid flows, and flows with drifting cylinders", *Computer Methods in Applied Mechanics and Engineering*, **94** (1992) 353–371, doi: 10.1016/0045-7825(92)90060-W.
7. T.E. Tezduyar, "Computation of moving boundaries and interfaces and stabilization parameters", *International Journal for Numerical Methods in Fluids*, **43** (2003) 555–575, doi: 10.1002/fld.505.
8. T.E. Tezduyar and S. Sathe, "Modeling of fluid–structure interactions with the space–time finite elements: Solution techniques", *International Journal for Numerical Methods in Fluids*, **54** (2007) 855–900, doi: 10.1002/fld.1430.
9. K. Takizawa and T.E. Tezduyar, "Multiscale space–time fluid–structure interaction techniques", *Computational Mechanics*, **48** (2011) 247–267, doi: 10.1007/s00466-011-0571-z.
10. T.J.R. Hughes, "Multiscale phenomena: Green's functions, the Dirichlet-to-Neumann formulation, subgrid scale models, bubbles, and the origins of stabilized methods", *Computer Methods in Applied Mechanics and Engineering*, **127** (1995) 387–401.
11. T.J.R. Hughes, A.A. Oberai, and L. Mazzei, "Large eddy simulation of turbulent channel flows by the variational multiscale method", *Physics of Fluids*, **13** (2001) 1784–1799.
12. Y. Bazilevs, V.M. Calo, J.A. Cottrell, T.J.R. Hughes, A. Reali, and G. Scovazzi, "Variational multiscale residual-based turbulence modeling for large eddy simulation of incompressible flows", *Computer Methods in Applied Mechanics and Engineering*, **197** (2007) 173–201.
13. Y. Bazilevs and I. Akkerman, "Large eddy simulation of turbulent Taylor–Couette flow using isogeometric analysis and the residual–based variational multiscale method", *Journal of Computational Physics*, **229** (2010) 3402–3414.
14. K. Takizawa, B. Henicke, T.E. Tezduyar, M.-C. Hsu, and Y. Bazilevs, "Stabilized space–time computation of wind-turbine rotor aerodynamics", *Computational Mechanics*, **48** (2011) 333–344, doi: 10.1007/s00466-011-0589-2.
15. T.J.R. Hughes, W.K. Liu, and T.K. Zimmermann, "Lagrangian–Eulerian finite element formulation for incompressible viscous flows", *Computer Methods in Applied Mechanics and Engineering*, **29** (1981) 329–349.
16. T. Tezduyar, S. Aliabadi, M. Behr, A. Johnson, and S. Mittal, "Parallel finite-element computation of 3D flows", *Computer*, **26** (1993) 27–36, doi: 10.1109/2.

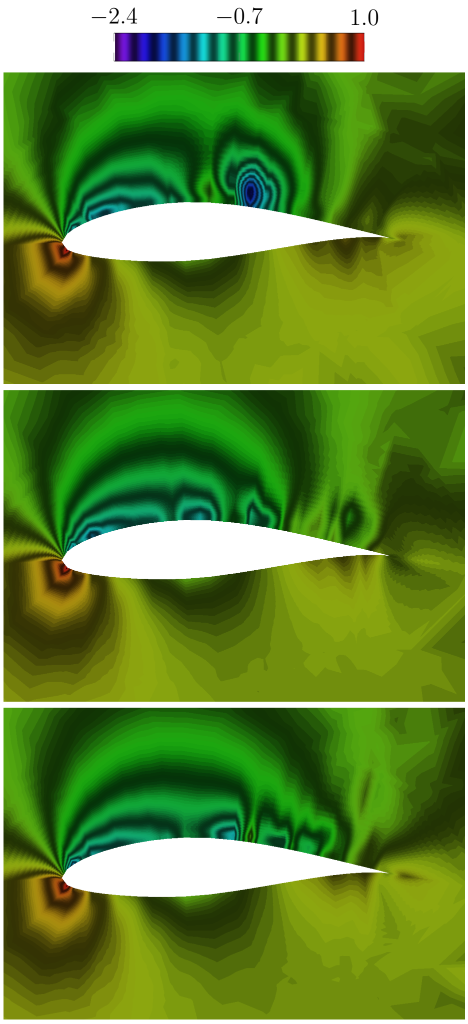

Fig. 15 Pressure coefficient at $t = 1.0$ s for Patch 16 (at $0.90R$). DSD/SST-DP-SUPS. Top: Mesh-2. Middle: Mesh-3. Bottom: Mesh-4.

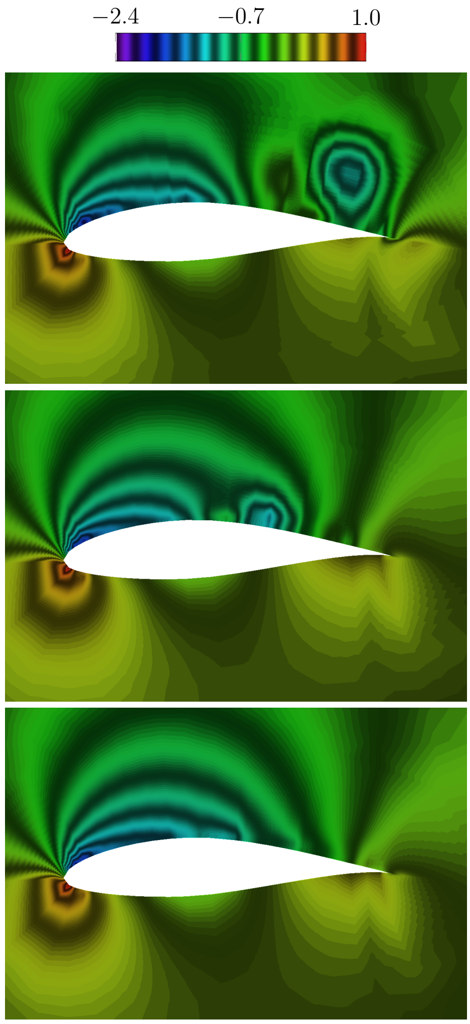

Fig. 16 Pressure coefficient at $t = 1.0$ s for Patch 16 (at $0.90R$). DSD/SST-DP-VMST (TGI). Top: Mesh-2. Middle: Mesh-3. Bottom: Mesh-4.

237441.

17. M. Behr, A. Johnson, J. Kennedy, S. Mittal, and T. Tezduyar, "Computation of incompressible flows with implicit finite element implementations on the Connection Machine", *Computer Methods in Applied Mechanics and Engineering*, **108** (1993) 99–118, doi: 10.1016/0045-7825(93)90155-Q.
18. T.E. Tezduyar, S.K. Aliabadi, M. Behr, and S. Mittal, "Massively parallel finite element simulation of compressible and incompressible flows", *Computer Methods in Applied Mechanics and Engineering*, **119** (1994) 157–177, doi: 10.1016/0045-7825(94)00082-4.
19. S. Mittal and T.E. Tezduyar, "Massively parallel finite element computation of incompressible flows involving fluid-body interactions", *Computer Methods in Applied Mechanics and Engineering*, **112** (1994) 253–282, doi: 10.1016/0045-7825(94)90029-9.
20. S. Mittal and T.E. Tezduyar, "Parallel finite element simulation of 3D incompressible flows – Fluid-structure interactions", *International Journal for Numerical Methods in Fluids*, **21** (1995) 933–953, doi: 10.1002/fld.1650211011.
21. S.K. Aliabadi and T.E. Tezduyar, "Parallel fluid dynamics computations in aerospace applications", *International Journal for Numerical Methods in Fluids*, **21** (1995) 783–805, doi: 10.1002/fld.1650211003.
22. T. Tezduyar, S. Aliabadi, M. Behr, A. Johnson, V. Kalro, and M. Litke, "Flow simulation and high performance computing", *Computational Mechanics*, **18** (1996) 397–412, doi: 10.1007/BF00350249.
23. A.A. Johnson and T.E. Tezduyar, "Parallel computation of incompressible flows with complex geometries", *International Journal for Numerical Methods in Fluids*, **24** (1997) 1321–1340, doi: 10.1002/(SICI)1097-0363(199706)24:12<1321::AID-FLD562>3.3.CO;2-C.
24. A.A. Johnson and T.E. Tezduyar, "Advanced mesh generation and update methods for 3D flow simulations", *Computational Mechanics*, **23** (1999) 130–143, doi: 10.1007/s004660050393.
25. M. Behr and T. Tezduyar, "The Shear-Slip Mesh Update Method", *Computer Methods in Applied Mechanics and Engineering*, **174** (1999) 261–274, doi: 10.1016/S0045-7825(98)00299-0.

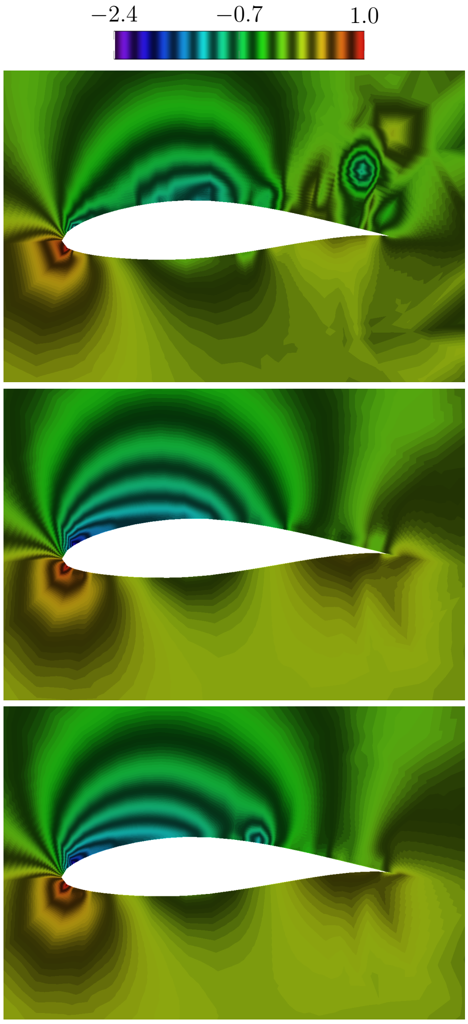

Fig. 17 Pressure coefficient at $t = 1.0$ s for Patch 16 (at $0.90R$). Top: DSD/SST-DP-SUPS (w/LSIC). Middle: DSD/SST-DP-VMST (TC2). Bottom: DSD/SST-DP-VMST (LHC).

26. V. Kalro and T.E. Tezduyar, "A parallel 3D computational method for fluid–structure interactions in parachute systems", *Computer Methods in Applied Mechanics and Engineering*, **190** (2000) 321–332, doi: 10.1016/S0045-7825(00)00204-8.
27. K. Stein, R. Benney, V. Kalro, T.E. Tezduyar, J. Leonard, and M. Accorsi, "Parachute fluid–structure interactions: 3-D Computation", *Computer Methods in Applied Mechanics and Engineering*, **190** (2000) 373–386, doi: 10.1016/S0045-7825(00)00208-5.
28. T.E. Tezduyar, "Finite element methods for flow problems with moving boundaries and interfaces", *Archives of Computational Methods in Engineering*, **8** (2001) 83–130, doi: 10.1007/BF02897870.
29. T. Tezduyar and Y. Osawa, "Fluid–structure interactions of a parachute crossing the far wake of an aircraft", *Computer Methods in Applied Mechanics and Engineering*, **191** (2001) 717–726, doi: 10.1016/S0045-7825(01)00311-5.
30. K. Stein, R. Benney, T. Tezduyar, and J. Potvin, "Fluid–structure interactions of a cross parachute: Numerical simulation", *Computer Methods in Applied Mechanics and Engineering*, **191** (2001) 673–687, doi: 10.1016/S0045-7825(01)00312-7.
31. R. Ohayon, "Reduced symmetric models for modal analysis of internal structural-acoustic and hydroelastic-sloshing systems", *Computer Methods in Applied Mechanics and Engineering*, **190** (2001) 3009–3019.
32. M. Behr and T. Tezduyar, "Shear-slip mesh update in 3D computation of complex flow problems with rotating mechanical components", *Computer Methods in Applied Mechanics and Engineering*, **190** (2001) 3189–3200, doi: 10.1016/S0045-7825(00)00388-1.
33. K. Stein, T. Tezduyar, and R. Benney, "Mesh moving techniques for fluid–structure interactions with large displacements", *Journal of Applied Mechanics*, **70** (2003) 58–63, doi: 10.1115/1.1530635.
34. K. Stein, T.E. Tezduyar, and R. Benney, "Automatic mesh update with the solid-extension mesh moving technique", *Computer Methods in Applied Mechanics and Engineering*, **193** (2004) 2019–2032, doi: 10.1016/j.cma.2003.12.046.
35. E.H. van Brummelen and R. de Borst, "On the nonnormality of subiteration for a fluid-structure interaction problem", *SIAM Journal on Scientific Computing*, **27** (2005) 599–621.
36. T.E. Tezduyar, S. Sathe, R. Keedy, and K. Stein, "Space–time finite element techniques for computation of fluid–structure interactions", *Computer Methods in Applied Mechanics and Engineering*, **195** (2006) 2002–2027, doi: 10.1016/j.cma.2004.09.014.
37. T.E. Tezduyar, S. Sathe, and K. Stein, "Solution techniques for the fully-discretized equations in computation of fluid–structure interactions with the space–time formulations", *Computer Methods in Applied Mechanics and Engineering*, **195** (2006) 5743–5753, doi: 10.1016/j.cma.2005.08.023.
38. R. Torii, M. Oshima, T. Kobayashi, K. Takagi, and T.E. Tezduyar, "Computer modeling of cardiovascular fluid–structure interactions with the Deforming-Spatial-Domain/Stabilized Space–Time formulation", *Computer Methods in Applied Mechanics and Engineering*, **195** (2006) 1885–1895, doi: 10.1016/j.cma.2005.05.050.
39. R. Torii, M. Oshima, T. Kobayashi, K. Takagi, and T.E. Tezduyar, "Fluid–structure interaction modeling of aneurysmal conditions with high and normal blood pressures", *Computational Mechanics*, **38** (2006) 482–490, doi: 10.1007/s00466-006-0065-6.
40. Y. Bazilevs, V.M. Calo, Y. Zhang, and T.J.R. Hughes, "Isogeometric fluid–structure interaction analysis with applications to arterial blood flow", *Computational Mechanics*, **38** (2006) 310–322.
41. R.A. Khurram and A. Masud, "A multiscale/stabilized formulation of the incompressible Navier–Stokes equations for moving boundary flows and fluid–structure interaction", *Computational Mechanics*, **38** (2006) 403–416.
42. T.E. Tezduyar, "Finite elements in fluids: Stabilized formulations and moving boundaries and interfaces", *Computers & Fluids*, **36** (2007) 191–206, doi: 10.1016/j.compfluid.2005.02.011.
43. T.E. Tezduyar, S. Sathe, T. Cragin, B. Nanna, B.S. Conklin, J. Pausewang, and M. Schwaab, "Modeling of fluid–structure interactions with the space–time finite elements: Arterial fluid mechanics", *International Journal for Numerical Methods in Fluids*, **54** (2007) 901–922, doi: 10.1002/fld.1443.
44. R. Torii, M. Oshima, T. Kobayashi, K. Takagi, and T.E. Tezduyar, "Influence of wall elasticity in patient-specific hemodynamic simulations", *Computers & Fluids*, **36** (2007) 160–168, doi: 10.1016/j.compfluid.

2005.07.014.
45. T. Sawada and T. Hisada, “Fluid–structure interaction analysis of the two dimensional flag-in-wind problem by an interface tracking ALE finite element method”, *Computers & Fluids*, **36** (2007) 136–146.
46. K. Takizawa, T. Yabe, Y. Tsugawa, T.E. Tezduyar, and H. Mizoe, “Computation of free–surface flows and fluid–object interactions with the CIP method based on adaptive meshless Soroban grids”, *Computational Mechanics*, **40** (2007) 167–183, doi: 10.1007/s00466-006-0093-2.
47. K. Takizawa, K. Tanizawa, T. Yabe, and T.E. Tezduyar, “Ship hydrodynamics computations with the CIP method based on adaptive Soroban grids”, *International Journal for Numerical Methods in Fluids*, **54** (2007) 1011–1019, doi: 10.1002/fld.1466.
48. T. Yabe, K. Takizawa, T.E. Tezduyar, and H.-N. Im, “Computation of fluid–solid and fluid–fluid interfaces with the CIP method based on adaptive Soroban grids — An overview”, *International Journal for Numerical Methods in Fluids*, **54** (2007) 841–853, doi: 10.1002/fld.1473.
49. R. Torii, M. Oshima, T. Kobayashi, K. Takagi, and T.E. Tezduyar, “Numerical investigation of the effect of hypertensive blood pressure on cerebral aneurysm — Dependence of the effect on the aneurysm shape”, *International Journal for Numerical Methods in Fluids*, **54** (2007) 995–1009, doi: 10.1002/fld.1497.
50. M. Manguoglu, A.H. Sameh, T.E. Tezduyar, and S. Sathe, “A nested iterative scheme for computation of incompressible flows in long domains”, *Computational Mechanics*, **43** (2008) 73–80, doi: 10.1007/s00466-008-0276-0.
51. T.E. Tezduyar, S. Sathe, J. Pausewang, M. Schwaab, J. Christopher, and J. Crabtree, “Interface projection techniques for fluid–structure interaction modeling with moving-mesh methods”, *Computational Mechanics*, **43** (2008) 39–49, doi: 10.1007/s00466-008-0261-7.
52. T.E. Tezduyar, S. Sathe, M. Schwaab, J. Pausewang, J. Christopher, and J. Crabtree, “Fluid–structure interaction modeling of ringsail parachutes”, *Computational Mechanics*, **43** (2008) 133–142, doi: 10.1007/s00466-008-0260-8.
53. T.E. Tezduyar, S. Sathe, M. Schwaab, and B.S. Conklin, “Arterial fluid mechanics modeling with the stabilized space–time fluid–structure interaction technique”, *International Journal for Numerical Methods in Fluids*, **57** (2008) 601–629, doi: 10.1002/fld.1633.
54. S. Sathe and T.E. Tezduyar, “Modeling of fluid–structure interactions with the space–time finite elements: Contact problems”, *Computational Mechanics*, **43** (2008) 51–60, doi: 10.1007/s00466-008-0299-6.
55. R. Torii, M. Oshima, T. Kobayashi, K. Takagi, and T.E. Tezduyar, “Fluid–structure interaction modeling of a patient-specific cerebral aneurysm: Influence of structural modeling”, *Computational Mechanics*, **43** (2008) 151–159, doi: 10.1007/s00466-008-0325-8.
56. Y. Bazilevs, V.M. Calo, T.J.R. Hughes, and Y. Zhang, “Isogeometric fluid–structure interaction: theory, algorithms, and computations”, *Computational Mechanics*, **43** (2008) 3–37.
57. J.G. Isaksen, Y. Bazilevs, T. Kvamsdal, Y. Zhang, J.H. Kaspersen, K. Waterloo, B. Romner, and T. Ingebrigtsen, “Determination of wall tension in cerebral artery aneurysms by numerical simulation”, *Stroke*, **39** (2008) 3172–3178.
58. W.G. Dettmer and D. Peric, “On the coupling between fluid flow and mesh motion in the modelling of fluid–structure interaction”, *Computational Mechanics*, **43** (2008) 81–90.
59. Y. Bazilevs and T.J.R. Hughes, “NURBS-based isogeometric analysis for the computation of flows about rotating components”, *Computational Mechanics*, **43** (2008) 143–150.
60. T.E. Tezduyar, M. Schwaab, and S. Sathe, “Sequentially-Coupled Arterial Fluid–Structure Interaction (SCAFSI) technique”, *Computer Methods in Applied Mechanics and Engineering*, **198** (2009) 3524–3533, doi: 10.1016/j.cma.2008.05.024.
61. R. Torii, M. Oshima, T. Kobayashi, K. Takagi, and T.E. Tezduyar, “Fluid–structure interaction modeling of blood flow and cerebral aneurysm: Significance of artery and aneurysm shapes”, *Computer Methods in Applied Mechanics and Engineering*, **198** (2009) 3613–3621, doi: 10.1016/j.cma.2008.08.020.
62. M. Manguoglu, A.H. Sameh, F. Saied, T.E. Tezduyar, and S. Sathe, “Preconditioning techniques for nonsymmetric linear systems in the computation of incompressible flows”, *Journal of Applied Mechanics*, **76** (2009) 021204, doi: 10.1115/1.3059576.
63. Y. Bazilevs, J.R. Gohean, T.J.R. Hughes, R.D. Moser, and Y. Zhang, “Patient-specific isogeometric fluid–structure interaction analysis of thoracic aortic blood flow due to implantation of the Jarvik 2000 left ventricular assist device”, *Computer Methods in Applied Mechanics and Engineering*, **198** (2009) 3534–3550.
64. Y. Bazilevs, M.-C. Hsu, D. Benson, S. Sankaran, and A. Marsden, “Computational fluid–structure interaction: Methods and application to a total cavopulmonary connection”, *Computational Mechanics*, **45** (2009) 77–89.
65. K. Takizawa, J. Christopher, T.E. Tezduyar, and S. Sathe, “Space–time finite element computation of arterial fluid–structure interactions with patient-specific data”, *International Journal for Numerical Methods in Biomedical Engineering*, **26** (2010) 101–116, doi: 10.1002/cnm.1241.
66. K. Takizawa, C. Moorman, S. Wright, J. Christopher, and T.E. Tezduyar, “Wall shear stress calculations in space–time finite element computation of arterial fluid–structure interactions”, *Computational Mechanics*, **46** (2010) 31–41, doi: 10.1007/s00466-009-0425-0.
67. T.E. Tezduyar, K. Takizawa, C. Moorman, S. Wright, and J. Christopher, “Multiscale sequentially-coupled arterial FSI technique”, *Computational Mechanics*, **46** (2010) 17–29, doi: 10.1007/s00466-009-0423-2.
68. R. Torii, M. Oshima, T. Kobayashi, K. Takagi, and T.E. Tezduyar, “Influence of wall thickness on fluid–structure interaction computations of cerebral aneurysms”, *International Journal for Numerical Methods in Biomedical Engineering*, **26** (2010) 336–347, doi: 10.1002/cnm.1289.
69. M. Manguoglu, K. Takizawa, A.H. Sameh, and T.E. Tezduyar, “Solution of linear systems in arterial fluid mechanics computations with boundary layer mesh refinement”, *Computational Mechanics*, **46** (2010) 83–89, doi: 10.1007/s00466-009-0426-z.
70. R. Torii, M. Oshima, T. Kobayashi, K. Takagi, and T.E. Tezduyar, “Role of 0D peripheral vasculature model in fluid–structure interaction modeling of aneurysms”, *Computational Mechanics*, **46** (2010) 43–52, doi: 10.1007/s00466-009-0439-7.
71. Y. Bazilevs, M.-C. Hsu, Y. Zhang, W. Wang, X. Liang, T. Kvamsdal, R. Brekken, and J. Isaksen, “A fully-coupled fluid–structure interaction simulation of cerebral aneurysms”, *Computational Mechanics*, **46** (2010) 3–16.
72. T.E. Tezduyar, K. Takizawa, C. Moorman, S. Wright, and J. Christopher, “Space–time finite element computation of complex fluid–structure interactions”, *In-*

ternational Journal for Numerical Methods in Fluids*, **64** (2010) 1201–1218, doi: 10.1002/fld.2221.
73. Y. Bazilevs, M.-C. Hsu, Y. Zhang, W. Wang, T. Kvamsdal, S. Hentschel, and J. Isaksen, "Computational fluid–structure interaction: Methods and application to cerebral aneurysms", *Biomechanics and Modeling in Mechanobiology*, **9** (2010) 481–498.
74. J. Kiendl, Y. Bazilevs, M.-C. Hsu, R. Wüchner, and K.-U. Bletzinger, "The bending strip method for isogeometric analysis of Kirchhoff–Love shell structures comprised of multiple patches", *Computer Methods in Applied Mechanics and Engineering*, **199** (2010) 2403–2416.
75. K. Takizawa, C. Moorman, S. Wright, T. Spielman, and T.E. Tezduyar, "Fluid–structure interaction modeling and performance analysis of the Orion spacecraft parachutes", *International Journal for Numerical Methods in Fluids*, **65** (2011) 271–285, doi: 10.1002/fld.2348.
76. K. Takizawa, C. Moorman, S. Wright, J. Purdue, T. McPhail, P.R. Chen, J. Warren, and T.E. Tezduyar, "Patient-specific arterial fluid–structure interaction modeling of cerebral aneurysms", *International Journal for Numerical Methods in Fluids*, **65** (2011) 308–323, doi: 10.1002/fld.2360.
77. K. Takizawa, S. Wright, C. Moorman, and T.E. Tezduyar, "Fluid–structure interaction modeling of parachute clusters", *International Journal for Numerical Methods in Fluids*, **65** (2011) 286–307, doi: 10.1002/fld.2359.
78. M. Manguoglu, K. Takizawa, A.H. Sameh, and T.E. Tezduyar, "Nested and parallel sparse algorithms for arterial fluid mechanics computations with boundary layer mesh refinement", *International Journal for Numerical Methods in Fluids*, **65** (2011) 135–149, doi: 10.1002/fld.2415.
79. T.E. Tezduyar, K. Takizawa, T. Brummer, and P.R. Chen, "Space–time fluid–structure interaction modeling of patient-specific cerebral aneurysms", *International Journal for Numerical Methods in Biomedical Engineering*, **27** (2011) 1665–1710, doi: 10.1002/cnm.1433.
80. K. Takizawa, T. Spielman, and T.E. Tezduyar, "Space–time FSI modeling and dynamical analysis of spacecraft parachutes and parachute clusters", *Computational Mechanics*, **48** (2011) 345–364, doi: 10.1007/s00466-011-0590-9.
81. K. Takizawa, T. Spielman, C. Moorman, and T.E. Tezduyar, "Fluid–structure interaction modeling of spacecraft parachutes for simulation-based design", *Journal of Applied Mechanics*, **79** (2012) 010907, doi: 10.1115/1.4005070.
82. K. Takizawa, T. Brummer, T.E. Tezduyar, and P.R. Chen, "A comparative study based on patient-specific fluid–structure interaction modeling of cerebral aneurysms", *Journal of Applied Mechanics*, **79** (2012) 010908, doi: 10.1115/1.4005071.
83. K. Takizawa, B. Henicke, A. Puntel, T. Spielman, and T.E. Tezduyar, "Space–time computational techniques for the aerodynamics of flapping wings", *Journal of Applied Mechanics*, **79** (2012) 010903, doi: 10.1115/1.4005073.
84. T. Tezduyar, S. Aliabadi, and M. Behr, "Enhanced-Discretization Interface-Capturing Technique (EDICT) for computation of unsteady flows with interfaces", *Computer Methods in Applied Mechanics and Engineering*, **155** (1998) 235–248, doi: 10.1016/S0045-7825(97)00194-1.
85. J.E. Akin, T.E. Tezduyar, and M. Ungor, "Computation of flow problems with the mixed interface-tracking/interface-capturing technique (MITICT)", *Computers & Fluids*, **36** (2007) 2–11, doi: 10.1016/j.compfluid.2005.07.008.
86. M.A. Cruchaga, D.J. Celentano, and T.E. Tezduyar, "A numerical model based on the Mixed Interface-Tracking/Interface-Capturing Technique (MITICT) for flows with fluid–solid and fluid–fluid interfaces", *International Journal for Numerical Methods in Fluids*, **54** (2007) 1021–1030, doi: 10.1002/fld.1498.
87. A.N. Brooks and T.J.R. Hughes, "Streamline upwind/Petrov-Galerkin formulations for convection dominated flows with particular emphasis on the incompressible Navier-Stokes equations", *Computer Methods in Applied Mechanics and Engineering*, **32** (1982) 199–259.
88. T.E. Tezduyar, S. Mittal, S.E. Ray, and R. Shih, "Incompressible flow computations with stabilized bilinear and linear equal-order-interpolation velocity-pressure elements", *Computer Methods in Applied Mechanics and Engineering*, **95** (1992) 221–242, doi: 10.1016/0045-7825(92)90141-6.
89. T.E. Tezduyar and Y.J. Park, "Discontinuity capturing finite element formulations for nonlinear convection-diffusion-reaction equations", *Computer Methods in Applied Mechanics and Engineering*, **59** (1986) 307–325, doi: 10.1016/0045-7825(86)90003-4.
90. T.E. Tezduyar and Y. Osawa, "Finite element stabilization parameters computed from element matrices and vectors", *Computer Methods in Applied Mechanics and Engineering*, **190** (2000) 411–430, doi: 10.1016/S0045-7825(00)00211-5.
91. J.E. Akin, T. Tezduyar, M. Ungor, and S. Mittal, "Stabilization parameters and Smagorinsky turbulence model", *Journal of Applied Mechanics*, **70** (2003) 2–9, doi: 10.1115/1.1526569.
92. J.E. Akin and T.E. Tezduyar, "Calculation of the advective limit of the SUPG stabilization parameter for linear and higher-order elements", *Computer Methods in Applied Mechanics and Engineering*, **193** (2004) 1909–1922, doi: 10.1016/j.cma.2003.12.050.
93. L. Catabriga, A.L.G.A. Coutinho, and T.E. Tezduyar, "Compressible flow SUPG parameters computed from element matrices", *Communications in Numerical Methods in Engineering*, **21** (2005) 465–476, doi: 10.1002/cnm.759.
94. A. Corsini, F. Rispoli, A. Santoriello, and T.E. Tezduyar, "Improved discontinuity-capturing finite element techniques for reaction effects in turbulence computation", *Computational Mechanics*, **38** (2006) 356–364, doi: 10.1007/s00466-006-0045-x.
95. L. Catabriga, A.L.G.A. Coutinho, and T.E. Tezduyar, "Compressible flow SUPG parameters computed from degree-of-freedom submatrices", *Computational Mechanics*, **38** (2006) 334–343, doi: 10.1007/s00466-006-0033-1.
96. F. Rispoli, A. Corsini, and T.E. Tezduyar, "Finite element computation of turbulent flows with the discontinuity-capturing directional dissipation (DCDD)", *Computers & Fluids*, **36** (2007) 121–126, doi: 10.1016/j.compfluid.2005.07.004.
97. L. Catabriga, D.A.F. de Souza, A.L.G.A. Coutinho, and T.E. Tezduyar, "Three-dimensional edge-based SUPG computation of inviscid compressible flows with YZβ shock-capturing", *Journal of Applied Mechanics*, **76** (2009) 021208, doi: 10.1115/1.3062968.
98. A. Corsini, C. Iossa, F. Rispoli, and T.E. Tezduyar, "A DRD finite element formulation for computing turbulent reacting flows in gas turbine combustors", *Computational Mechanics*, **46** (2010) 159–167, doi: 10.1007/s00466-009-0441-0.

99. M.-C. Hsu, Y. Bazilevs, V.M. Calo, T.E. Tezduyar, and T.J.R. Hughes, “Improving stability of stabilized and multiscale formulations in flow simulations at small time steps”, *Computer Methods in Applied Mechanics and Engineering*, **199** (2010) 828–840, doi: 10.1016/j.cma.2009.06.019.
100. A. Corsini, F. Rispoli, and T.E. Tezduyar, “Stabilized finite element computation of NOx emission in aero-engine combustors”, *International Journal for Numerical Methods in Fluids*, **65** (2011) 254–270, doi: 10.1002/fld.2451.
101. J. Jonkman, S. Butterfield, W. Musial, and G. Scott, “Definition of a 5-MW reference wind turbine for offshore system development”, Technical Report NREL/TP-500-38060, National Renewable Energy Laboratory, 2009.
102. D.A. Spera, “Introduction to modern wind turbines”, in D.A. Spera, editor, *Wind Turbine Technology: Fundamental Concepts of Wind Turbine Engineering*, 47–72, ASME Press, 1994.
103. Y. Saad and M. Schultz, “GMRES: A generalized minimal residual algorithm for solving nonsymmetric linear systems”, *SIAM Journal of Scientific and Statistical Computing*, **7** (1986) 856–869.
104. G. Karypis and V. Kumar, “A fast and high quality multilevel scheme for partitioning irregular graphs”, *SIAM Journal of Scientific Computing*, **20** (1998) 359–392.